

CREEP CRACK GROWTH PARAMETERS FOR DIRECTIONALLY SOLIDIFIED SUPERALLOYS

B. Gardner¹, A. Saxena², J. Qu¹

¹G.W.Woodruff School of Mechanical Engineering

²School of Materials Science and Engineering

Georgia Institute of Technology

Atlanta, 30332-0245, USA

ABSTRACT

Crack tip parameters used in nonlinear fracture mechanics are examined using finite element simulations for characterizing high temperature crack growth in directionally solidified (DS) Ni-base superalloys. The anisotropy in these materials is modeled as orthotropic materials in which the plastic and creep properties are different along the longitudinal and transverse directions. The elastic behavior of the material is modeled as isotropic. The loading direction is chosen along the longitudinal axis of the grains and the crack is located in the transverse plane. The analysis shows that $C(t)$ characterizes the crack tip stress and strain as a function of time and also the evolution of the creep zone size and shape during the small-scale creep conditions. This leads to the conclusion that the parameters that characterize the crack growth rate in isotropic materials such as C^* and C_t are also suitable for DS materials for Mode I cracks when the loading axis coincides with one of the main material axis.

KEYWORDS: creep, fatigue, crack, DS Ni – alloys, C_t , C^*

INTRODUCTION

The performance of natural gas-fired gas turbines has steadily improved with the continuous development of advanced materials and design concepts for hot gas path components. The use of directionally solidified (DS) superalloy with adequate coatings has significantly improved the limitations inherent to equiaxed materials in the areas of oxidation and corrosion resistance, thermal and low cycle fatigue resistance, creep resistance and high cycle fatigue resistance [1]. A major aspect of any design or remaining (or residual) life assessment methodology for high temperature components is the ability to predict the creep and creep-fatigue crack growth behavior in these materials. This requires the use of nonlinear fracture mechanics concepts.

Directionally solidified materials by design are anisotropic because grain sizes in the longitudinal direction can be on the order of 100 mm and on the order of only a few mm in the transverse and the short transverse directions. The tensile and the creep data clearly show significant differences in the plastic and creep deformation behavior in the longitudinal and transverse directions. Thus, it is perhaps more accurate to represent them as orthotropic materials in which the creep deformation properties in the direction along the grain axis differ substantially from the properties in the transverse direction.

The crack tip parameters currently used for predicting creep and creep-fatigue crack growth are based on the assumptions that the material is isotropic. The purpose of this paper is to use finite element simulations to

explore the applicability and limitations of crack tip parameters such as C^* , C_t and $C(t)$ for predicting crack growth in DS materials.

CRACK TIP PARAMETERS FOR CREEP CRACK GROWTH

We assume power-law creep behavior and that a cracked body is subjected to a static load under creep conditions and the load has been applied for sufficiently long time so that steady-state creep develops over the entire remaining ligament. Under these circumstances, the C^* -integral is shown to uniquely characterize the crack tip stress and strain rates through the Hutchinson-Rice-Rosengren (HRR) fields [2]. The C^* -Integral is defined as [2]:

$$C^* = \int_{\Gamma} W^* dy - T_i (\partial \dot{u}_i / \partial x) ds \quad (1)$$

Where, Γ = a path that originates on the lower crack surface and ends on the upper crack surface enclosing the crack tip, \dot{u}_i = displacement rate, T_i = components of the traction vector, W^* = stress-power density, ds = incremental distance along the path, Γ .

The validity of the C^* -integral is limited to extensive steady-state creep conditions. In practice, this condition may not always be realized because components contain stress and temperature gradients and are designed to resist widespread creep deformation. Therefore, it is necessary to derive the crack tip stress fields for the conditions of small-scale creep (SSC) and the transition creep (TC). Under SSC, the creep zone is restricted to a small region near the crack tip and is much smaller than the length dimensions such as crack size and the remaining ligament, and the surrounding material is under elastic conditions. Riedel and Rice [3] and Ohji, Ogura and Kubo [4] independently derived the nature of the crack tip stress fields under small-scale creep conditions as a function of time. The above analysis lends itself to the estimation of the creep zone size and transition time, t_T , which is the time needed for extensive creep conditions to develop from SSC conditions. Riedel and Rice [3] defined the creep zone boundary as the locus of points where time-dependent effective creep strains equal the instantaneous effective elastic strains in the cracked body. The transition time is the time when the small-scale-creep stress fields equal to the extensive steady-state creep fields characterized by C^* .

Bassani and McClintock [5] recognized that the crack tip stress fields under SSC can also be characterized by a time-dependent $C(t)$ -integral, whose value is determined along a contour taken very close to the crack tip. $C(t)$ is same as C^* except its value is determined close to the crack tip within a region where the creep strains dominate over the elastic strains. In contrast, the value of C^* can be determined along any contour which originates at the lower crack surface and ends on the upper crack surface enclosing the crack tip. Thus, determining the $C(t)$ -integral requires accurate solutions of stress and strain near the crack tip. Bassani and McClintock [5] further related the value of $C(t)$ with the HRR type stress fields. The validity of the $C(t)$ -integral is not simply limited to the small-scale creep conditions because $C(t)$ becomes equal to C^* for extensive steady-state creep with the additional property that its value becomes path-independent. Hence, $C(t)$ can be said to be the amplitude of the HRR field for all conditions ranging from small-scale to extensive secondary-state creep and also including the transition creep conditions, in between. Therefore, to investigate time-dependent crack tip stress fields in DS materials, we will focus on the $C(t)$ -integral and its value determined along a path taken very close to the crack tip.

C_t parameter [2] is different from $C(t)$ in that it is uniquely related the stress power dissipation rate and the rate of expansion of the creep zone size in the small-scale-creep regime. In the extensive creep regime, C_t , $C(t)$ and C^* all become identical by definition. The advantage of C_t over $C(t)$ in the small-scale-creep regime is that it can be measured at the loading pins while $C(t)$ cannot. Therefore, C_t has been widely used for correlating creep crack growth data over a wide range of conditions ranging from small-scale-creep to extensive creep [2]. The relationship between C_t and the rate of expansion of the creep zone size, \dot{r}_c is given by the following equation [2]:

$$C_t = \frac{2K^2(1-\nu^2)}{EW} \beta (F'/F) \dot{r}_c \quad (2)$$

Where, K = stress intensity factor, W = specimen width, E = elastic modulus, ν = Poisson's ratio, F = K -calibration function, F' = first derivative of F with respect to (a/W) , and β = constant with a value of

approximately 0.33. The creep zone size in the above equation is referenced to its extent along 90 degrees from the crack plane.

FINITE ELEMENT ANALYSIS OF ORTHOTROPIC MATERIALS

In this study, the DS material is modeled as isotropic elastic and orthotropic creep with different creep properties in the longitudinal and transverse directions. The finite element method is used to investigate the development of the creep zone and to calculate the magnitude of $C(t)$ for a stationary crack.

The orthotropic creep behavior was implemented in the numerical model using Hill's anisotropic yield function. The anisotropic yield function contains 6 constants for general loading. If we restrict loading to the principal axes, the number of constants can be reduced to three. The loading of the model is applied such that the principal axes are coincident with the longitudinal and transverse directions of the directionally solidified alloy. The equivalent deviatoric stress function based on Hill's anisotropic yield function in principal stress space is

$$\tilde{q}(\sigma) = \left[F(\sigma_2 - \sigma_3)^2 + G(\sigma_3 - \sigma_1)^2 + H(\sigma_1 - \sigma_2)^2 \right]^{1/2} \quad (3)$$

where, F , G , and H are coefficients associated with the anisotropic creep properties.

The equivalent steady-state creep relationship is

$$\dot{\varepsilon}_{cr} = A \tilde{q}^n \quad (4)$$

Where, $\dot{\varepsilon}_{cr}$ is the equivalent steady-state creep rate, A is the equivalent creep coefficient, and n is the creep exponent. The constants F , G , and H are determined using the creep coefficients from three uniaxial creep tests, one in each of the principal directions. Substituting the equivalent deviatoric stress for each of the uniaxial creep tests yield

$$\dot{\varepsilon}_{icr} = A_i \sigma_i^n = A \tilde{q}^n \quad (5)$$

Where, $i=1,2,3$, $\dot{\varepsilon}_{icr}$ is the steady-state creep rate in the i -direction, A_i is the creep exponent in the i -direction, σ_i is the i^{th} principal stress, and n is the creep exponent. It is important to note that the use of this approach allows for different creep coefficients to accommodate the material anisotropy, but the creep exponent must be the same for each direction. Combining Eq. (3) and Eq. (5) for each of the uniaxial test yields the following relationships between the anisotropic creep coefficients and the equivalent creep coefficient.

$$\begin{aligned} A_x &= (G + H)^{n/2} A \\ A_y &= (F + H)^{n/2} A \\ A_z &= (F + G)^{n/2} A \end{aligned} \quad (6)$$

By setting $A=A_x$, the following equations are obtained for F , G , and H

$$\begin{aligned} F &= \frac{1}{2} \left[\left(\frac{A_y}{A_x} \right)^{2/n} + \left(\frac{A_z}{A_x} \right)^{2/n} - 1 \right] \\ G &= \frac{1}{2} \left[\left(\frac{A_z}{A_x} \right)^{2/n} + 1 - \left(\frac{A_y}{A_x} \right)^{2/n} \right] \\ H &= \frac{1}{2} \left[\left(\frac{A_y}{A_x} \right)^{2/n} + 1 - \left(\frac{A_z}{A_x} \right)^{2/n} \right] \end{aligned} \quad (7)$$

A finite element model of a standard compact type (CT) specimen was created. The finite element model is 2-d, plane strain and consists of 15413 nodes and 4988 8-noded quadrilateral elements, Figure 1. Crack tip elements are used to ensure accurate representation of the stress and strain field at the crack tip. The use of crack tip elements is particularly important in the calculation of $C(t)$ because its value is only valid as the dimension of the contour around the crack tip approaches zero. A detailed figure of the crack tip mesh is shown in Figure 2. A load of 2000 N is applied to the finite element model through the semi-rigid loading pins and the a/W ratio is 0.5. The stress intensity factor for this configuration is $109.2 \text{ MPa(m)}^{1/2}$. The finite

element model was analyzed using ABAQUS, which includes the anisotropic creep model based on Hill's function among its standard routines.

RESULTS

Three different finite element models were evaluated for comparison: isotropic ($A_x=A_y$), orthotropic - longitudinal bias ($A_y > A_x$), and orthotropic - transverse bias ($A_x > A_y$). The creep coefficient is 1.06×10^{-14} MPa⁻⁶/hr and the creep exponent is 6 for the isotropic case. Using a load of 2000 N, the corresponding transition time is 430 hours for the isotropic case. The coefficients for the orthotropic models are shown in Table 1.

Table 1 – Orthotropic Creep Properties for Finite Element Model

	A_x (MPa ⁻⁶ /hr)	A_y (MPa ⁻⁶ /hr)	A_z (MPa ⁻⁶ /hr)
Long. Bias	1.061×10^{-14}	4.897×10^{-14}	1.061×10^{-14}
Trans. Bias	1.061×10^{-14}	2.290×10^{-15}	2.290×10^{-15}

Figure 3 shows the resulting creep zone at 500 hours for all three finite element models. In this figure, the creep zone is defined as the boundary where the equivalent creep strain is equal to the largest principal elastic strain. The crack tip parameter $C(t)$ was calculated during the finite element simulation. A plot of $C(t)$ versus time for each of the three finite element models is presented in Figure 4. The most important result from this plot is the fact that the value of $C(t)$ approaches a unique value as time increases for the two orthotropic cases evaluated. In the isotropic case, it is well known that $C(t) \rightarrow C^*$ as $t \rightarrow \infty$. This result shows that $C(t)$ -Integral can be used for characterization of crack tip stress under extensive creep conditions for DS materials.

Figure 5 shows the development of the creep zone for the orthotropic – transverse bias ($A_x > A_y$) case. The results of the analytical study showed the creep zone does in fact grow in a self-similar fashion even with the orthotropic creep properties. Figure 6 shows a plot of the creep zone size as a function of time on a log-log scale for angles of 90 and 45 degrees from the crack plane. A line of slope of $2/(n-1) = 0.4$ for $n=6$ is plotted through the data to compare the numerical results to the analytically predicted slope [2,3]. The good agreement between the numerical and analytical values attests to the validity of C_t for uniquely characterizing the creep zone expansion rate. This result has significant implications in regard to the use of C_t [6] parameter for characterizing the creep crack growth behavior in DS materials.

CONCLUSIONS

Finite element analyses of compact type specimens subjected to sustained load conditions made from orthotropic materials with different creep properties along the major axes show that crack tip stress and strain fields as a function of time and the evolution of the crack tip creep zone size and shape are characterized by the $C(t)$ -Integral. Thus, the foundation has been laid for the use of parameters such as C^* and C_t for characterizing high temperature crack growth.

REFERENCES

1. Stringer, J. and Viswanathan, R., (1993) "Gas Turbine Hot-Section Materials and Coatings in Electric Utility Applications", Proceedings of ASM Materials Congress, Pittsburgh, 1.
2. Saxena, A., (1998) Nonlinear Fracture Mechanics for Engineers, CRC Press.
3. Riedel, H. and Rice, J.R., (1980), ASTM Special Technical Publication, STP 700, 112.
4. Ohji, K., Ogura, K., and Kubo, S., (1979), Transactions of Japan Society of Mechanical Engineering, 790-13, 18.
5. Bassani, J.L. and McClintock, F.A., (1981), International Journal of Solids and Structures, 17, 79.
6. Saxena, A. (1986), ASTM Special Technical Publication, STP 905, 185.

ACKNOWLEDGEMENTS

The authors wish to acknowledge the financial support of the General Electric Power Systems Company for the financial support of this study.

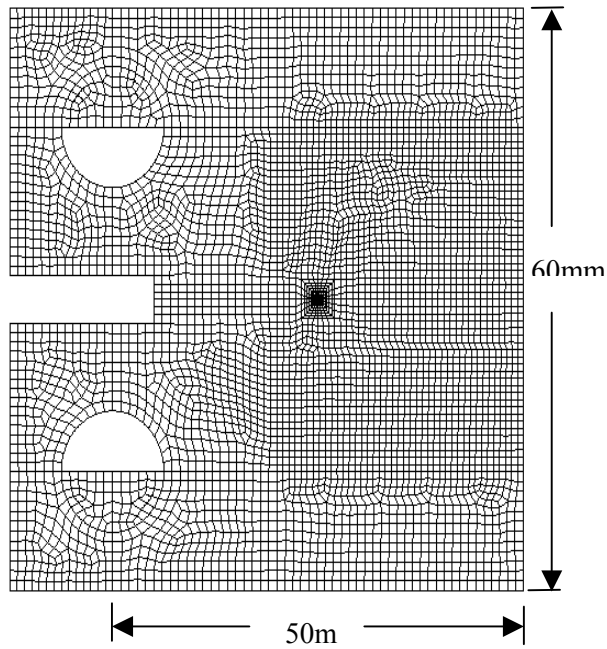


Figure 1: Finite Element Model of CT Specimen

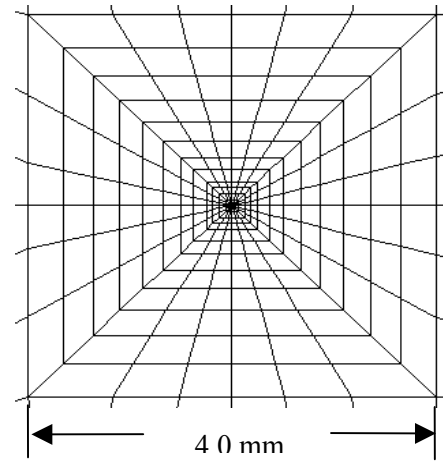


Figure 2: Close-Up View of Crack Tip Region in Finite Element Model

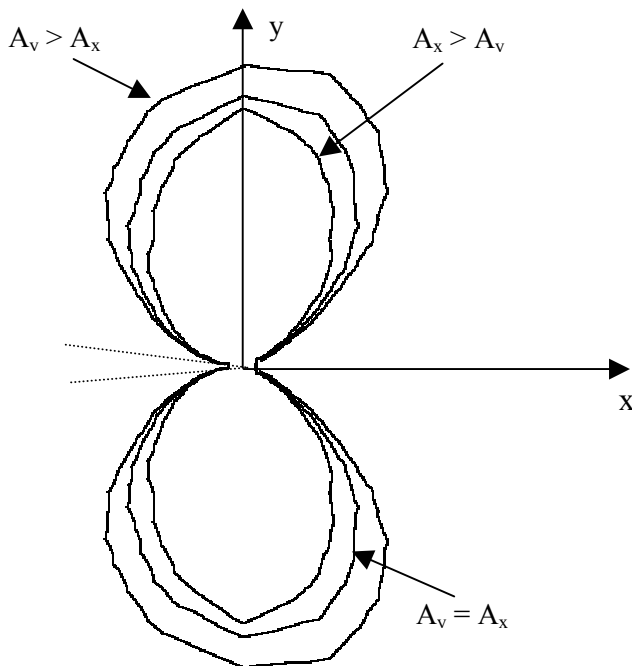


Figure 3: Boundary of creep zone at $t=500\text{hr}$ for all three finite element models

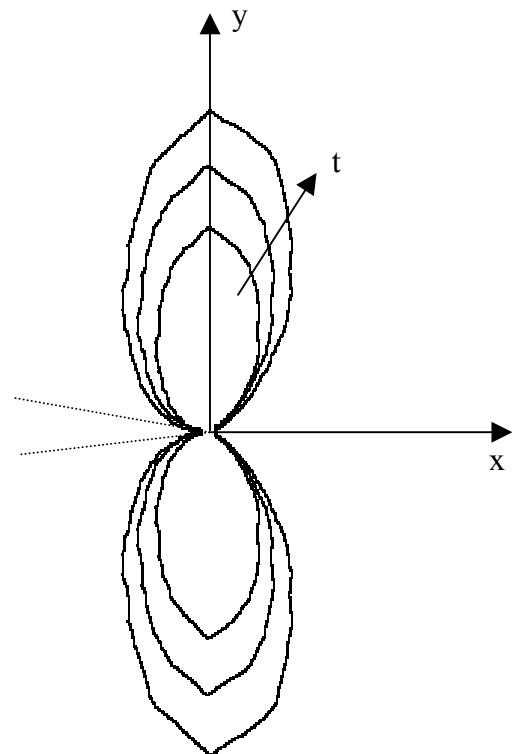


Figure 4: Evolution of Creep Zone for Orthotropic - Transverse Bias Case ($t=200, 500, 1000\text{ hr}$)

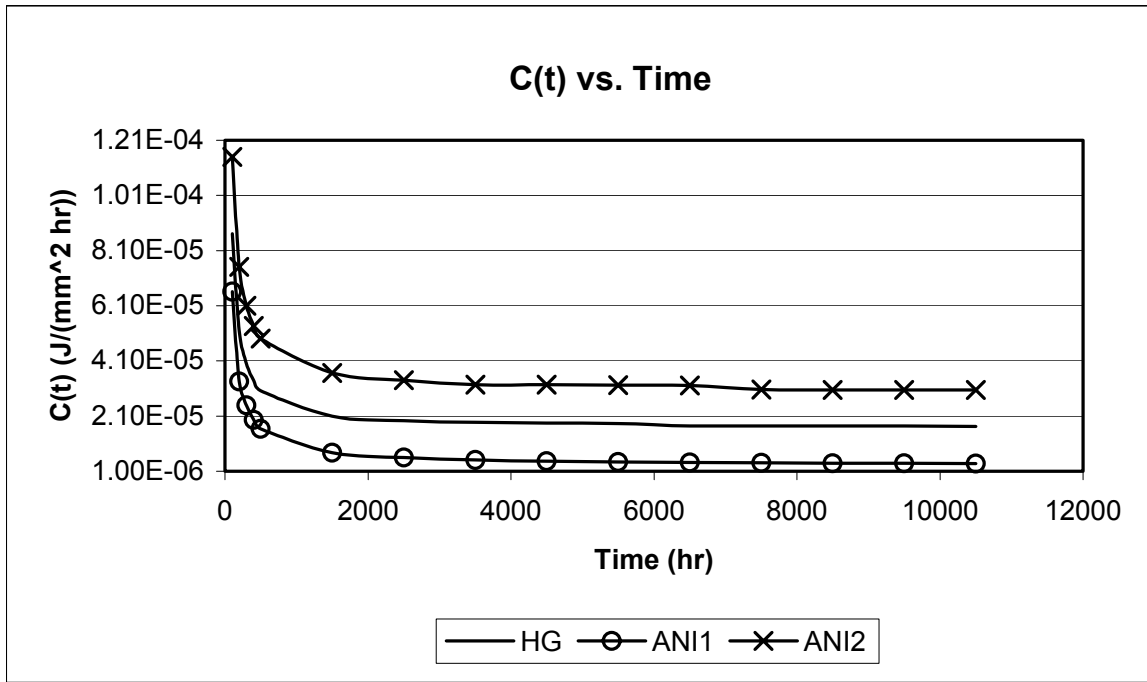


Figure 5: Comparison of $C(t)$ vs. Time for each of the three finite element models

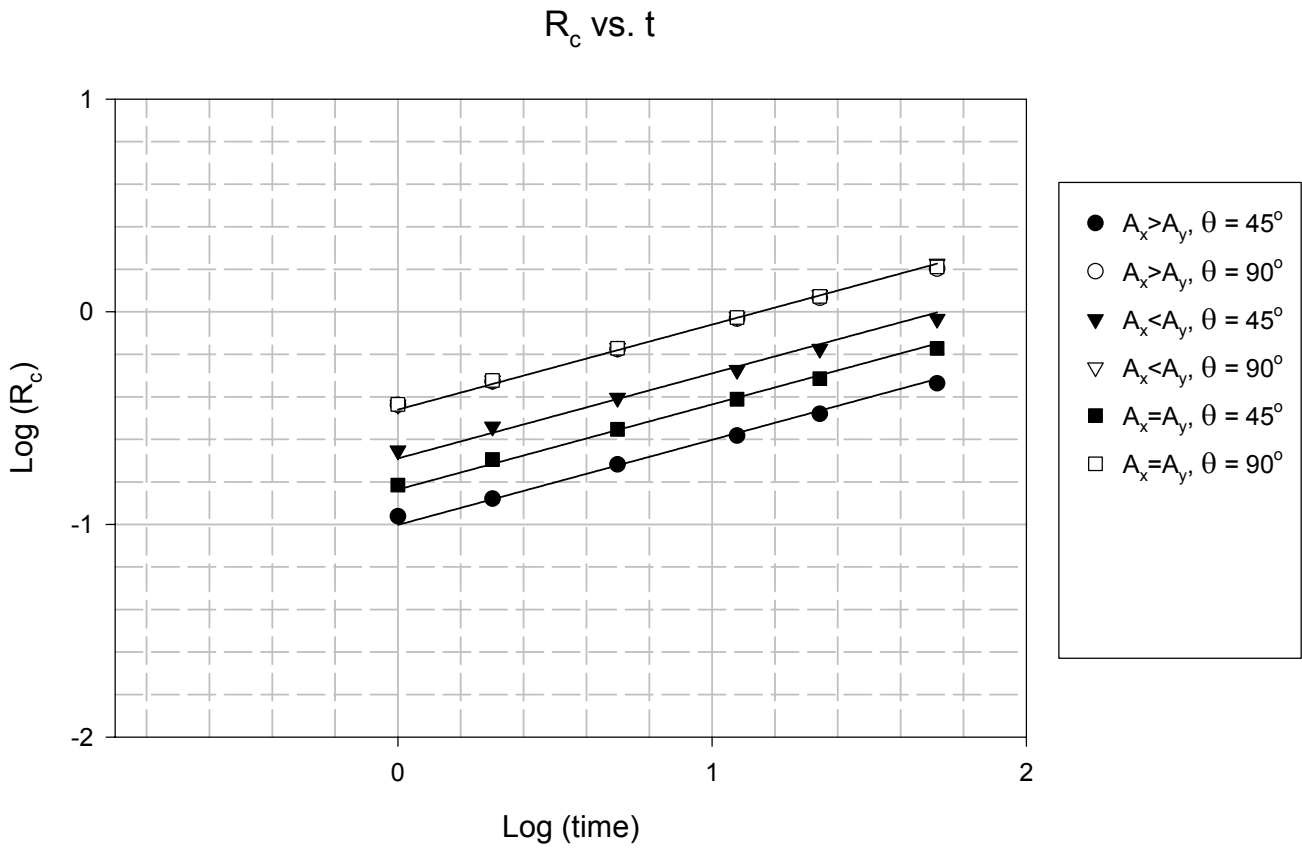


Figure 6: Plot of Creep Zone Radius vs. Time for angles of $\theta = 45^\circ$ and $\theta = 90^\circ$